Journal of Power Sources 226 (2013) 71–74

Contents lists available at SciVerse ScienceDirect

Journal of Power Sources

journal homepage: www.elsevier.com/locate/jpowsour

Short communication

Ball-milling assisted solid-state reaction synthesis of mesoporous $Li_4Ti_5O_{12}$ for lithium-ion batteries anode

Chao Lai [a], ZhenZhen Wu [a], YuXuan Zhu [a], QingDuan Wu [b,**], Liang Li [a], Chao Wang [a,*]

[a] School of Chemistry and Chemical Engineering, and Jiangsu Key Laboratory of Green Synthetic Chemistry for Functional Materials, Jiangsu Normal University, Xuzhou, Jiangsu 221116, China
[b] China National Academy of Nanotechnology & Engineering, Teda, Tianjin 300457, China

HIGHLIGHTS

- Mesoporous $Li_4Ti_5O_{12}$ is prepared via ball-milling assisted solid-state reaction.
- $Li_4Ti_5O_{12}$ consists of ultrafine nanoparticles and well-defined mesopores.
- The as-prepared sample shows good high-rate and cycle performance.
- The route could be practical for the mass synthesis of $Li_4Ti_5O_{12}$ anodes.

ARTICLE INFO

Article history:
Received 29 September 2012
Received in revised form
25 October 2012
Accepted 30 October 2012
Available online 7 November 2012

Keywords:
Mesoporous
Lithium titanate
Lithium-ion batteries
High-rate
Solid-state reaction

ABSTRACT

Mesoporous $Li_4Ti_5O_{12}$ is prepared via ball-milling assisted solid-state reaction with titanyl sulfate and LiOH as precursors. Different from previous reports, the solid-state reaction route generates mesopores in $Li_4Ti_5O_{12}$ by removing the impurities after the high-temperature synthesis process. This technique ensures the formation of well-defined mesoporous structure and ultrafine nanoparticles with the size of around 8 nm. The as-prepared sample shows good rate and cycle performance. At the current density of 1750 mA g^{-1} (10 C), high initial discharge capacity of 174.5 mAh g^{-1} can be obtained, which can be retained at 143.4 mAh g^{-1} after 50 cycles. This facile ball-milling assisted solid-state reaction could be a practical way for the mass synthesis of mesoporous $Li_4Ti_5O_{12}$ as high-performance anodes.

1. Introduction

Potential applications of lithium-ion batteries in electric vehicles and hybrid electric vehicles have spurred extensive research to develop novel electrode materials with improved safety and long cycle life [1,2]. Spinel $Li_4Ti_5O_{12}$ has been suggested as one of the most promising alternatives for graphite anode, as it demonstrates zero structural change during the charge–discharge process to ensure a stable cycle performance and a high potential around 1.5 V to avoid the formation of solid-electrolyte interphase (SEI) layer [3–9]. Despite these advantages, $Li_4Ti_5O_{12}$ still suffers from the problem of poor high-rate performance arising from its low electrical conductivity (10^{-13} S cm^{-1}). To conquer this problem, considerable efforts have been made; and one of the most effective strategies is to fabricate nanostructured $Li_4Ti_5O_{12}$ [3–10]. By reducing the particle dimensions to nanoscale, the distance of electron and lithium-ion transport is shorten, and the contact area between electrode and electrolyte is increased, which will lead to the improved electrochemical performance [3–9,11]. Among those different morphologies, mesoporous $Li_4Ti_5O_{12}$ is of particular interest, for it shows some additional appealing features. For example, the developed mesopores can facilitate the fast transport of solvated electrolyte and lithium ions throughout the electrode materials, and the high surface area can effectively reduce the current density per unit surface area [3–5,12–14].

Many strategies, which can be simply designated as solution methods and solid-state reaction process, have been developed to prepared mesoporous $Li_4Ti_5O_{12}$ [3–5,12–14]. Between these two processes, the solid-state reaction process is more competitive for

* Corresponding author. Tel.: +86 0516 83403003; fax: +86 0516 83403320.
** Corresponding author. Tel: +86 022 62002900; fax: +86 022 62002984.
E-mail addresses: qingduan_wu@cnane.com.cn (Q. Wu), wangc@jsnu.edu.cn, wangc@xznu.edu.cn (C. Wang).

0378-7753/$ – see front matter © 2012 Elsevier B.V. All rights reserved.
http://dx.doi.org/10.1016/j.jpowsour.2012.10.086

practical applications, as it can be scaled up for mass production with lower cost and less complicated process [15,16]. However, a high calcination temperature is required to obtain pure $Li_4Ti_5O_{12}$ in a conventional solid-state reaction, and this will lead to the collapse of nanopores, the generation of coarse particle size and inhomogeneous phase composition [8,15]. Therefore, it is very important to design a novel solid-state reaction route to prepare mesoporous $Li_4Ti_5O_{12}$.

In this work, a facile ball-milling assisted solid-state reaction method has been developed prepare to $Li_4Ti_5O_{12}$ by employing titanyl sulfate and LiOH as precursor. The initial ball-milling step is employed to obtain titanate and Li_2SO_4, which is then calcined to fabricate $Li_4Ti_5O_{12}$ with Li_2SO_4 as the impurity. While the conventional pore-forming process is carried out before or during the calcination step [3–5,12–14], this novel solid-state reaction route utilizes the washing of Li_2SO4 to generate mesopores after the calcination process. A preliminary electrochemical measurement was carried out to demonstrate the high performance of the as-prepared mesoporous $Li_4Ti_5O_{12}$ sample.

2. Experimental

2.1. Preparation and characterization

To prepare pure $Li_4Ti_5O_{12}$, first, $TiOSO_4 \cdot xH_2O$ (4.02 g, $TiOSO_4$-93wt%, aladdin) and $LiOH \cdot H_2O$ (2.765 g, AR) were added in the agate tank and then well mixed by ball-milling, which was performed in a planetary ball mill (ZKX-2B, Nanjing) under air atmosphere at a speed of 300 rpm for 4 h. The resulting mixture was calcined at 500 °C for 2.5 h in a muffle furnace in air, and washed with water to remove impurities. After being dried at 60 °C for 24 h, mesoporous $Li_4Ti_5O_{12}$ can be obtained. For comparison, $Li_4Ti_5O_{12}$ was also prepared via the same process with a higher annealing temperature at 600 °C.

The as-prepared sample was characterized by X-ray diffraction (XRD, D8 Advance), Brunauer–Emmett–Teller (BET, Autosorb-1-mp) measurements, scanning electron microscopy (SEM, 1530vp), and transmission electron microscopy (TEM, JEM-2010FEF).

2.2. Electrochemical measurements

The working electrode was prepared by compressing a mixture of active materials, acetylene black, and binder (polytetrafluoroethylene, PTFE) in a weight ratio of 75:15:10. The weight of working electrode is around 3 mg. Lithium metal was used as the counter and reference electrodes. The electrolyte was LiPF6 (1 M) dissolved in a mixture of ethylene carbonate (EC), ethyl methyl carbonate (EMC) and dimethyl carbonate (DMC) with a volume ratio of 1:1:1. The galvanostatic method at the charge/discharge current density of 1750 mA g^{-1} (10 C) was employed to measure the electrochemical capacity and cycle life of the working electrode using a LAND-CT2001A instrument. The cut-off potentials for charge and discharge were set at 2.5 and 1.0 V (vs. Li^+/Li), respectively. All electrochemical measurements were carried out at room temperature.

3. Results and discussion

The ball-milling assisted solid-state reaction route can be simply divided into three steps: i) the ball-milling process to generate titanate and Li_2SO_4; ii) the annealing process to fabricate $Li_4Ti_5O_{12}$; iii) the washing process to produce mesopores. Herein, three advantages of this facile method can be identified: i) the generation of titanate can help decrease the formation temperature of $Li_4Ti_5O_{12}$; ii) the existence of Li_2SO_4 can restrict the rapid growth of $Li_4Ti_5O_{12}$ during the calcination process; iii) the developed mesopores can be simply produced by washing away the Li_2SO_4 impurity. Accordingly, XRD patterns of $Li_4Ti_5O_{12}$ prepared at different temperature are given in Fig. 1. All the peaks can be indexed as the spinel phase structure, suggesting the formation of pure $Li_4Ti_5O_{12}$ [3–9,12–17]. There is no difference between the diffraction peaks for the samples prepared at 500 and 600 °C. It is clear that a lower temperature is enough to fabricate pure $Li_4Ti_5O_{12}$.

To reveal the morphologies of as-prepared $Li_4Ti_5O_{12}$, typical SEM images are presented in Fig. 2a–d. As shown, both samples are fragmented particles and no obvious difference is found. For the sample annealed at 600 °C, it is obvious that microsized $Li_4Ti_5O_{12}$ are assembled with primary nanoparticles, and porous structure can be observed. However, for the sample annealed at 500 °C, the detailed microstructure is not clearly revealed in the SEM images due to its small size as shown in the TEM images in Fig. 2e and f. It can be seen that $Li_4Ti_5O_{12}$ prepared at 500 °C is also the agglomerates of nanoparticles with a size of around 8 nm, and obvious growth of particle size can be observed for the sample prepared at 600 °C. Different fringe spacings can be detected in the HRTEM image. The two interference fringe spacings are 0.21 nm and 0.48 nm, corresponding to the (400) and (111) plane of $Li_4Ti_5O_{12}$, respectively. The porous structure of both samples is further investigated by Brunauer–Emmett–Teller (BET) measurements. The N_2 adsorption–desorption isotherms and corresponding pore size distribution of the as-prepared $Li_4Ti_5O_{12}$ are shown in Fig. 3. All the samples show a typical Type IV isotherm, indicating the presence of mesoporous structure [12–14]. It is also demonstrated from the desorption branches of the isotherm that $Li_4Ti_5O_{12}$ annealed at 500 °C have predominant mesopores centered at 1.9 and 3.8 nm, and the large specific surface area of about 153.7 m^2 g^{-1} is also obtained. For the sample annealed at 600 °C, the pore size is increased, and the surface area is decreased to 77.6 m^2 g^{-1}. Obviously, the heat treatment has a large effect on the change of the surface area. For the sample annealed at 500 °C, the developed mesoporous structure and small particle size around 8 nm make it a very promising candidate for electrode materials with excellent high-rate discharge capability.

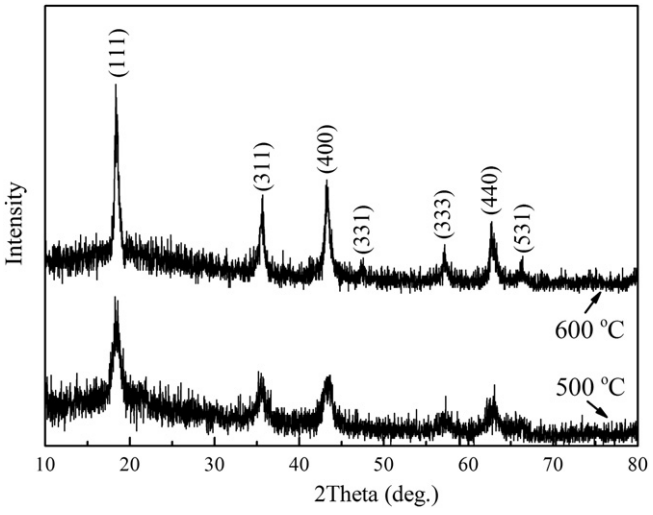

Fig. 1. XRD patterns of as-prepared $Li_4Ti_5O_{12}$ at different temperatures.

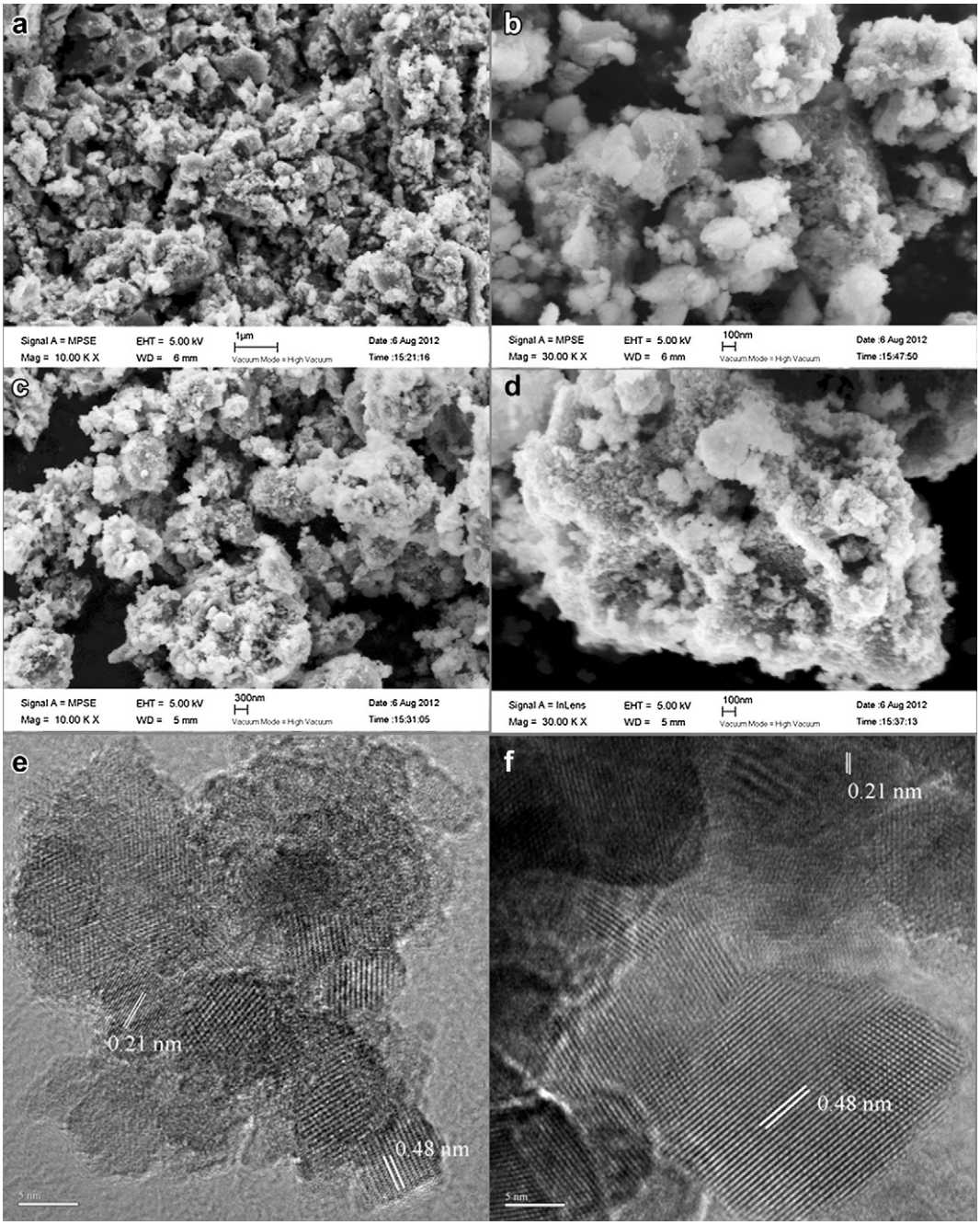

Fig. 2. SEM and TEM images of as-prepared $Li_4Ti_5O_{12}$ annealed at 500 °C (a, b, e) and 600 °C (c, d, f).

To evaluate the rate performance of as-prepared samples, cell tests were conducted and initial discharge–charge curves of $Li_4Ti_5O_{12}$ at the current density of 1750 mAh g^{-1} (10 C) are given in Fig. 4a. As shown, both samples demonstrate a distinct discharge and charge potential plateaus around 1.4 and 1.7 V. This is a typical character of two-phase co-existence of $Li_4Ti_5O_{12}/Li_7Ti_5O_{12}$, indicating the well development of crystalline phase of $Li_4Ti_5O_{12}$, in agreement with the XRD and TEM results [4–10,12–16]. The initial discharge and charge capacities of $Li_4Ti_5O_{12}$ annealed at 500 °C are about 174.5 and 152.7 mAh g^{-1}, implying nearly the entire electrode materials are electrochemically active. For the sample annealed at 600 °C, the discharge and charge capacity is just about 151.2 and 129.8 mAh g^{-1}. Moreover, it should be noted that both samples show an irreversible capacity of 20 mAh g^{-1} at the first discharge–charge cycle, and the relatively low columbic efficiency is attributed to the existence of irreversible Li trapped sites, which is widely reported for nanostructured materials [3–9,12–15]. Fig. 4b is the cycle curves of as-prepared $Li_4Ti_5O_{12}$ at the current density of 1750 mAh g^{-1}. It is obvious both samples demonstrate good cycle performance. After 50 cycles, the discharge capacity can be stably retained at 143.4 mAh g^{-1} for the sample prepared at 500 °C and at 124.4 mAh g^{-1} for the sample annealed at 600 °C. This excellent high-rate discharge and cycle performance for the sample prepared by the ball-milling assisted solid-state reaction method can be attributed to its ultrafine particle sizes and developed mesoporous structure.

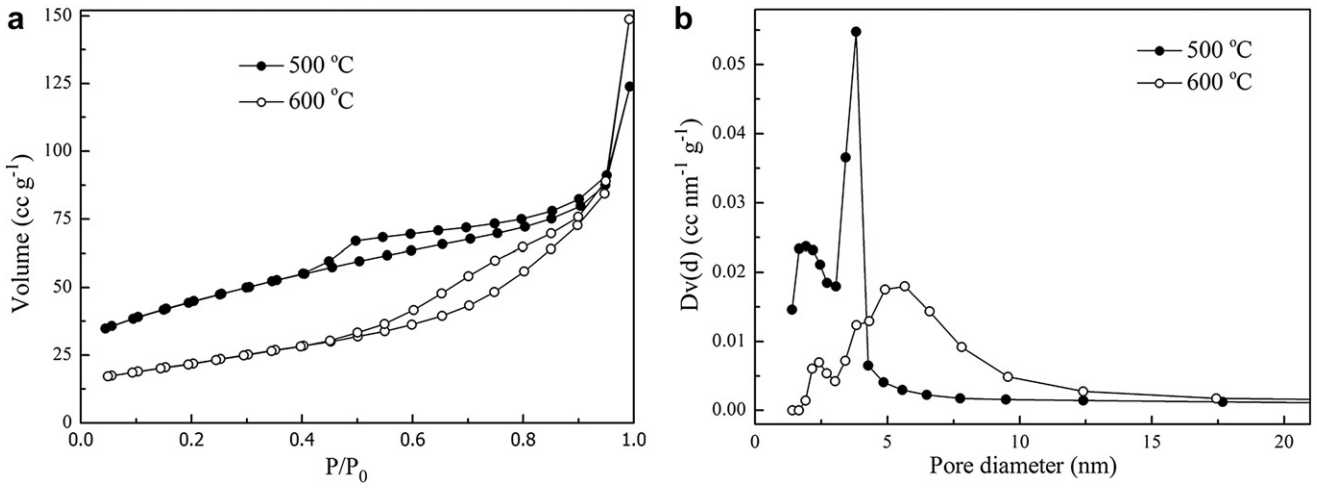

Fig. 3. N_2 adsorption–desorption isotherms (a) and corresponding pore size distribution (b) of the as-prepared $Li_4Ti_5O_{12}$ at different temperatures.

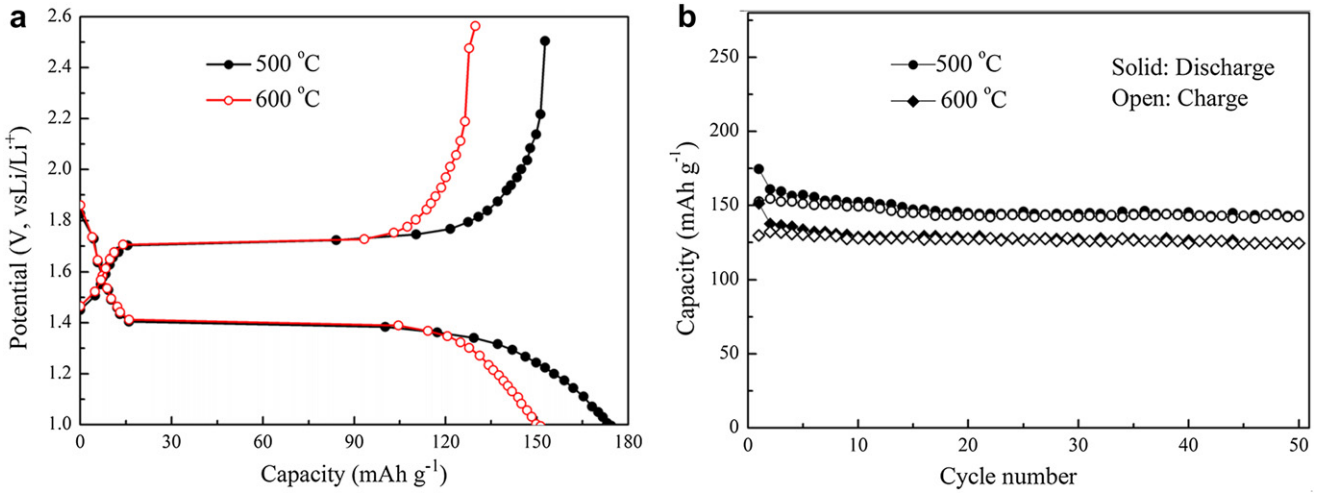

Fig. 4. Initial discharge–charge curves (a) and cycle performance (b) of as-prepared $Li_4Ti_5O_{12}$ at the current density of 1750 mA g^{-1}.

4. Conclusions

In summary, we have designed a novel ball-milling assisted solid-state reaction route, and successfully prepared mesoporous $Li_4Ti_5O_{12}$. The effect of annealing temperature on the structure and electrochemical performance of as-prepared $Li_4Ti_5O_{12}$ is both investigated. For the sample annealed at 500 °C, good rate performance is obtained, and the discharge capacity can be stably retained at 143.4 mAh g^{-1} after 50 cycles at the current density of 1750 mA g^{-1}, showing obvious advantages over the sample annealed at higher temperature. The ultrafine primary particles of around 8 nm in diameter and well developed mesoporous structure contribute to its good high-rate discharge capability.

Acknowledgments

This work has been supported by the Chinese National Science Funds (No. 21073153, No. 21173180 and No. 51202094); the Priority Academic Program Development of Jiangsu Higher Education Institutions; the Natural Science Foundation (No. 12KJB150010) of Jiangsu Education Committee of China; Jiangsu Qing-Lan Project (10QLD005).

References

[1] J.B. Goodenough, Y. Kim, Chem. Mater. 22 (2010) 587.
[2] J.-M. Tarascon, M. Armand, Nature 414 (2001) 359.
[3] L. Zhao, Y.S. Hu, H. Li, Z.X. Wang, L.Q. Chen, Adv. Mater. 23 (2011) 1385.
[4] J.Z. Chen, L. Yang, S.H. Fang, S. Hirano, K. Tachibana, J. Power Sources 200 (2012) 59.
[5] Y.S. Lin, J.G. Duh, J. Power Sources 196 (2011) 10698.
[6] K. Amine, I. Belharouak, Z.H. Chen, T. Tran, H. Yumoto, N. Ota, S.T. Myung, Y.K. Sun, Adv. Mater. 22 (2010) 3052.
[7] J. Lu, C.Y. Nan, Q. Peng, Y.D. Li, J. Power Sources 202 (2012) 246.
[8] S.L. Chou, J.Z. Wang, H.K. Liu, S.X. Dou, J. Phys. Chem. C 115 (2011) 16220.
[9] H.G. Jung, S.T. Myung, C.S. Yoon, S.B. Son, K.H. Oh, K. Amine, B. Scrosati, Y.K. Sun, Energy Environ. Sci. 4 (2011) 1345.
[10] K.M. Colbow, J.R. Dahn, R.R. Haering, J. Power Sources 26 (1989) 397.
[11] A.S. Arico, P. Bruce, B. Scrosati, J.M. Tarascon, W.V. Schalkwijk, Nat. Mater. 4 (2005) 366.
[12] G.N. Zhu, H.J. Liu, J.H. Zhuang, C.X. Wang, Y.G. Wang, Y.Y. Xia, Energy Environ. Sci. 4 (2011) 4016.
[13] E. Kang, Y.S. Jung, G.H. Kim, J.Y. Chun, U. Wiesner, A.C. Dillon, J.K. Kim, J. Lee, Adv. Funct. Mater. 21 (2011) 4349.
[14] Y.F. Tang, L. Yang, Z. Qiu, J.S. Huang, J. Mater. Chem. 19 (2009) 5980.
[15] T. Yuan, R. Cai, Z.P. Shao, J. Phys. Chem. C 115 (2011) 4943.
[16] Y.R. Jhan, J.G. Duh, J. Power Sources 198 (2012) 294.
[17] K. Ariyoshi, R. Yamato, T. Ohzuku, Electrochim. Acta 51 (2005) 1125.